

Effects of Combustion Model and Chemical Kinetics in Numerical Modeling of Hydrogen-Fueled Dual-Stage HVOF System

Sobhan Emami¹ · Hamed Jafari¹ · Yasser Mahmoudi²

Submitted: 13 June 2018 / in revised form: 26 November 2018 / Published online: 28 January 2019
© The Author(s) 2019

Abstract The present work examines the effect of utilizing different combustion models and chemical kinetics in predicting the properties of gas and particle phases in a hydrogen-fueled, dual-stage high-velocity oxy-fuel (HVOF) thermal spray system. For this purpose, effects of two combustion models, eddy dissipation concept (EDC) and eddy dissipation model (EDM), on the temperature and velocity fields in the system are studied. The computations using EDC model are performed for detailed and reduced chemical kinetics and for a range of mixture from lean to rich. It is found that EDC with multi-step reaction mechanism predicts higher temperatures for the flow and particle in the warm spray system. In contrast to EDC, the EDM with one-step global reaction shows extra heat release outside the HVOF barrel for rich mixtures which leads to unphysical higher prediction of particle temperature. The simulations using EDC model with detailed and reduced chemical kinetics show some exothermic reactions in converging-divergent nozzle of the system. The heat release from these reactions has profound impacts on the flow and particle temperatures and affects the gas dynamic behavior of flow considerably. Finally, it is discussed that moving toward rich mixtures is more reliable way to control the particles temperature.

Keywords chemical kinetics · dual-stage high-velocity oxy-fuel (HVOF) · eddy dissipation combustion model · hydrogen fuel

Introduction

The application of high-velocity oxygen-fuel (HVOF) thermal spray technique has been growing in the last two decades in many industries such as aerospace, automotive, oil and petrochemical, power generation, electronic, and medical science due to its excellent coating performance. Conventional single-stage HVOF systems are typically a high-pressure combustion chamber followed by a converging–diverging (C–D) nozzle. The system powered by gaseous fuel (like hydrogen, propylene, propane, acetylene and natural gas) or liquid fuel (like kerosene). In this system, the injected particles are accelerated and heated through a subsonic and then supersonic combusting gas flow and hit the substrate, which is placed at around 200–400 mm from nozzle exit (Ref 1). In order to form a dense, tough, uniform and high-quality layer of coating, proper temperature and velocity at the impact moment should be obtained (Ref 2). One negative point about HVOF system is the fact that it has no powerful control over the gas phase temperature and consequently the particle phase temperature. Furthermore, in HVOF system, desirable change in temperature can cause an undesirable change in other characteristics (e.g., velocity of particle and oxygen content of flow) (Ref 3). These shortcomings have more adverse impact on the phase-sensitive and temperature-sensitive materials like titanium and copper.

Dual-stage high-velocity oxygen-fuel (HVOF) thermal spray system, which is also called warm spray, was developed to overcome the shortcomings (i.e., no powerful

✉ Sobhan Emami
sobhan@pmc.iaun.ac.ir

Yasser Mahmoudi
s.mahmoudilarimi@qub.ac.uk

¹ Department of Mechanical Engineering, Najafabad Branch, Islamic Azad University, Najafabad, Iran

² School of Mechanical and Aerospace Engineering, Queen's University Belfast, Belfast BT9 5AH, UK

control over the gas and particle temperatures) of the single-stage HVOF system (Ref 4). The principles of warm spray are similar to HVOF process. As can be seen in Fig. 1, a converging nozzle followed by a mixing chamber is placed between combustion chamber and C–D nozzle. In the mixing chamber, different mass flow rates of nitrogen are added as coolant in order to dilute the hot gases. This can be known as the powerful temperature regulator in warm spray technique. Warm spray gun also has a barrel, which joins to the C–D nozzle, and particles are introduced to supersonic flow at barrel entrance. By such a design, warm spray gun can provide us with particle temperatures much lower than HVOF process, while the velocity of particle will be comparable with HVOF (Ref 1).

The processes in the HVOF guns are very complex and involve multi-phase turbulent flow, chemical reaction, heat transfer and supersonic/subsonic flow transition (Ref 5). Moreover, the influence of processing conditions on particle characteristics and coating quality is highly nonlinear and might not be thoroughly revealed by experimental studies (Ref 2). Hence, numerical techniques are effective tools and can provide an insight into the underlying momentum and heat transfer mechanisms (Ref 6, 7).

In the HVOF technology that is categorized as combustion-assisted thermal spray system, the quality of coating highly depends on the flame characteristics including its temperature, location, shape and emissions (Ref 8). Hence, in the numerical simulation of single- and dual-stage HVOF process, our approach to combustion modeling will be a determining factor. As it is reviewed by Li et al. (Ref 2), different approaches have been used to model the reaction rate in the literature, including: (1) laminar finite reaction rate model with Arrhenius expression (e.g., Ref 9–14), (2) infinitely fast reaction rate or chemical equilibrium (e.g., Ref 15–18) or frozen composition (Ref 5) at the domain and (3) finite reaction rate limited by turbulent mixing or eddy dissipation combustion model (EDM) (e.g., Ref 19–28).

By comparison between single-step and 12 steps reaction mechanism, Hassan et al. (Ref 12) demonstrated that a global single-step Arrhenius model adequately represents the combustion of propylene. However, for such a simple combustion model, adjustable model constants need to be calibrated consistent with the physics of the problem (Ref 13). In addition, it is discussed by Poinot and Veynante (Ref 29) that usual Arrhenius kinetics model implicitly assumes that the chemical time scales are larger than turbulent time scale. Thus, this model does not have reasonable accuracy in turbulent combustion application. That is why reaction rate closures in turbulent combustion are usually derived from physical analysis. In addition, Kamins and Gu (Ref 23) studied propane combustion in a HVOF thermal spray gun using three combustion models. They concluded that the flow pattern predicted by laminar finite reaction rate model could not be validated by experimental data.

Dolatabadi et al. (Ref 19) stated that in the HVOF thermal spray process, the rate of reaction is controlled by the rate of turbulent mixing and thus, knowledge of accurate Arrhenius rate data is not needed. Hence, they (Ref 19) claimed that the EDM describes the combustion process in HVOF gun adequately accurate. EDM is the most prevalent combustion model, which is utilized in simulation of single-stage HVOF and warm spray guns so far. However, there are some concerns with the numerical modeling of single-stage HVOF guns with EDM model. One of these is an under-prediction of particle temperature and velocity at the end of the computational domain in comparison with experimental data (Ref 8, 19). Khan and Shamim (Ref 26) utilized a single-step mechanism for propylene along with EDM combustion model and an improved turbulence model (i.e., RNG $k-\epsilon$) in order to validate the model against the experimental data of single-stage HVOF. Although the numerical results of particle velocity fit the experimental data, the particle temperature at the impact point is still much lower (around 400 K) than experimental

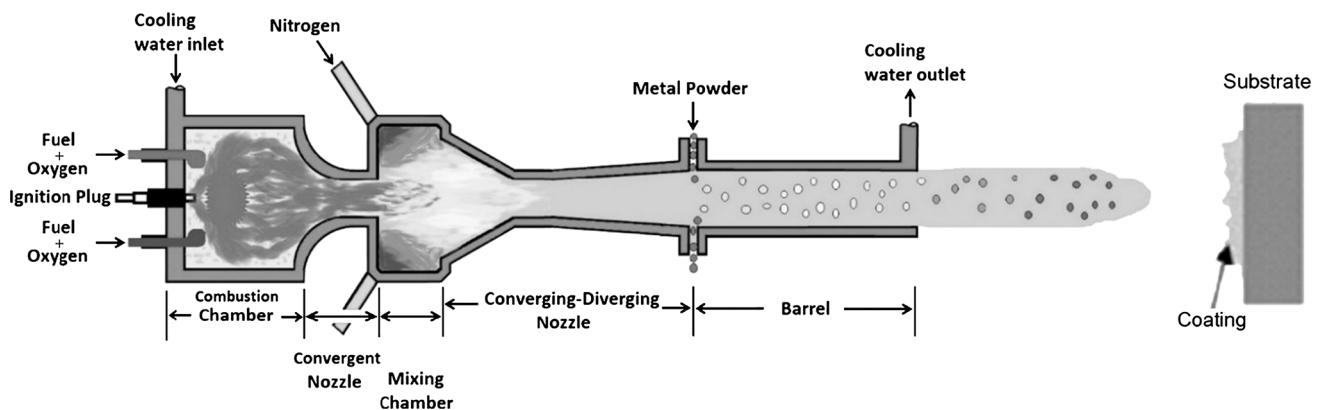


Fig. 1 Schematic diagram of a warm spray process (Ref 3)

values. The difference between numerical and experimental results in Ref 19 and 26 was related to the exothermic oxidation reaction between ambient air and particles which was ignored by numerical simulations. However, the weaknesses of models (i.e., combustion and turbulence models) utilized in these simulations might be another reason for this discrepancy between numerical and experimental results.

Another concern in using EDM, which is introduced in rich mixtures, is suspicious reaction between excessive unburned fuel and the oxygen diffused from ambient air into the core of jet flow outside of barrel (Ref 8, 27, 30). This phenomenon leads to a drastic increase in gas temperature and gives raise to particle temperature outside gun. The effect of fuel/oxygen (F/O) ratio on the performance of a dual-stage HVOF system was studied by Khan and Shamim (Ref 27) utilized propylene fuel gas along with EDM. Although the maximum gas temperature occurs in the slightly rich mixture, the particle temperature at the end of computational domain increases continuously as the fuel/oxygen (F/O) ratio increases. This finding is justified by exothermic reaction between unburned fuel and ambient air (Ref 27). The same observations are reported by Cheng et al. (Ref 18) for fuel-rich mixtures using an approximate equilibrium chemistry model. Nonetheless, based on the flow velocity, low concentration of fuel and oxygen, and gas phase temperature, occurrence of combustion in this region is very unlikely. Moreover, the experimental results reported by Turunen et al. (Ref 31) for a single-stage HVOF shows when the mixture is moving toward rich region the particle temperature decreases.

For this reason in the present work, we take the advantage of Eddy Dissipation Concept (EDC) (Ref 32) to model the turbulent combustion in HVOF process. In addition, to predict the reaction and heat release rate more accurately, the effect of detailed chemical mechanism is taken into account. Recently, Wang et al. (Ref 33) used a non-premixed combustion model to study the effect of fuel and oxygen inlet turbulent intensity, fuel droplet size and the oxygen/fuel ratio on the combustion and flow behavior in a kerosene-fueled single-stage HVOF gun. Unfortunately, they did not analyze the effect of this combustion model on the behavior of the particle phase. Therefore, it is not possible to draw conclusions on how a non-premixed combustion model can affect particle velocity and temperature in comparison with experimental data.

Another aim of the present paper is related to type of the fuel. While hydrogen is one of the most common fuels used in industrial HVOF guns (Ref 34), there is no numerical simulation in open literature to investigate the effect of utilizing this fuel on the performance of single- or dual-stage HVOF systems. Some experimental studies (Ref 31, 35) showed that using hydrogen fuel in a single-stage

HVOF typically results in greater velocity of the particle comparing with propane and propylene gases. Despite safety concerns about the usage of hydrogen, this gas has the unique characteristics like high energy density, a wide range of flammability limits and low emission, and free from soot.

The above literature review shows that the absence of a numerical investigation of hydrogen-fueled warm spray gun is still conspicuous since commercial hydrogen-fueled HVOF systems are so common; therefore, hydrogen can be a potential fuel for warm spray process. Furthermore, since EDM combustion model totally ignores the impact of chemistry, the present work will consider the impacts of chemical kinetics along with turbulent mixing by utilizing eddy dissipation concept (EDC) model in order to enhance numerical investigation of warm spray process and other combustion-assisted thermal spray processes. In summary:

1. This paper provides equivalence between a propylene-fueled warm spray system and a hydrogen-fueled one by considering reactant flow rate and stoichiometric ratio as variant parameters.
2. In the next stage, the results from EDC and EDM combustion models for hydrogen-fueled HVOF system are compared and a detailed discussion on necessity of considering the impact of chemistry is done.
3. Using the EDC model, we further discuss the effect of considering detailed and reduced chemical mechanisms on the numerical results.
4. Finally, we analyze the activation of secondary reactions inside the warm spray gun. In this section, the validity of previously claimed combustion reactions outside of the barrel due to diffusion of ambient air into the core of flow is further studied.

Numerical Model Description

Numerical Method

In the current study, the Eulerian formulation is used to solve the flow field and Lagrangian particle tracking method is utilized to provide particle flow characteristics. The particle phase is coupled with the gas phase, and the impact of particle loads on the gas phase is considered. It is revealed that the momentum and thermal impact of particle phase on the gas phase should be considered, otherwise the particle velocity and temperature will be calculated with error regardless of the amount of particle loads (Ref 3).

The governing equations in the gas phase, consist of compressible Favre (mass-weighted)-averaged form of mass, momentum, energy and species balance equations. The ideal gas equation of state couples the pressure and

density. In the particle phase, Newton's law governs the motion of the particle in the gas flow field. In the absence of Basset history term, gravitational force, thermophoresis force and forces caused by pressure gradient, the dominant force affecting the motion of the particle is the drag force (Ref 2). For drag coefficients, particles are supposed to be spherical. To investigate the effect of turbulent flow on particle motion, the discrete random walk model (DRW) or "eddy lifetime" model is used (Ref 25, 36). It is also showed that the Biot number of the particles is typically less than 0.1 (Ref 17), so that the particle internal resistance is ignored and the temperature gradient inside the particle is assumed to be zero. Thus, the heat transfer equation between a single particle and continuous gas phase is reduced to a first-order ordinary differential equation (ODE). The details of governing equations for gas and particle phases can be found in Ref 3.

The CFD commercial code ANSYS Fluent 16.1 is utilized to solve the governing equations. The solver performs under 2-D, axisymmetric, double-precision, steady-state and pressure-based conditions. The pressure and density are connected using the ideal gas state equation. Semi-Implicit Method for Pressure Linked Equations (SIMPLE) algorithm (Ref 37) is employed to treat pressure–velocity coupling. The second-order upwind discretization approach is utilized for all equations in order to avoid numerical diffusion.

Computational Domain and Boundary Conditions

The schematic diagram and the boundary conditions of a warm spray gun are shown in Fig. 2. The computational domain includes combustion chamber, converging nozzle, mixing chamber, C–D nozzle, barrel and finally atmosphere (where the substrate is located). A, B and C indicate inlets for fuel-oxygen, nitrogen and particle, respectively.

All wall temperatures are fixed at 350 K, and the entrance temperatures of fuel-oxygen, nitrogen and particle are assumed to be 300 K (Ref 26). The ambient pressure is also fixed at 1 atm. The particle diameter is 15 μm and other particle properties such as heat capacity and density

are taken from Ref 26. Table 1 also presents the working conditions of the warm spray.

Turbulence and Combustion Models

In the present work, the objective is to analyze the effect of different combustion models on the flow feature and performance of the system. Thus, in the following sections, we discuss turbulence and combustion models exploited in the present work.

Turbulence Model

The advanced Reynolds-stress turbulence model (RSM) along with the non-equilibrium wall function treatment is used to predict the turbulent eddy viscosity term that appears in the averaged form of momentum equation. The RSM closes the averaged Navier–Stokes equations by solving transport equations for the Reynolds stresses, together with an equation for the dissipation rate. This means that five additional transport equations are required in 2D flows (Ref 38). Since the RSM takes into account the effects of streamline curvature, swirl, rotation, and rapid changes in strain rate in a more rigorous manner than one-equation and two-equation models, it has greater potential to provide accurate predictions for complex flows (Ref 36). RSM predicts the mixing of burnt hot gases and cold nitrogen in the mixing chamber more accurately by abandoning the isotropic eddy viscosity hypothesis, which is utilized in other RANS turbulence model (Ref 25). By enforcing the wall y -plus between 30 and 300 in the current

Table 1 Operating conditions

Parameter	Value
Fuel + Oxygen mass flow rate	0.006740, kg/s
Nitrogen mass flow rate	0.008604, kg/s
Particle mass flow rate	0.00054, kg/s

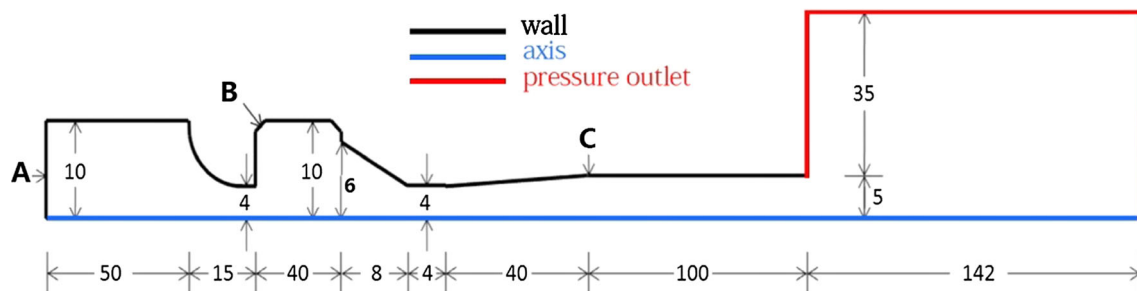


Fig. 2 Schematic diagram and boundary conditions of a typical warm spray gun (Ref 3). All dimensions are in mm

simulation, the non-equilibrium wall function treatment is utilized in order to deal with near wall flow.

Combustion Model

In the present research, both eddy dissipation model (EDM) and eddy dissipation concept (EDC) model are utilized and the results from these two models are compared and discussed. The EDM model developed by Magnussen and Hjertager (Ref 39) is the most common combustion model, which is utilized in previous study on simulation of single- and dual-stage HVOF guns (e.g., Ref 19-28). In this model, it is assumed that the reaction rate does not depend on chemical characteristics. Consequently, the combustion rate is mostly controlled by the turbulent characteristics of the flow field. In other words, in the premixed combustion, turbulent flow breaks down eddies containing unburned gasses into smaller ones with enough interfaces with hot gases to facilitate heat conduction and molecular mixing. In the next step, the reactions are completed at the mixing moment. In EDM, average concentration of species and the turbulent intensity in the flow are the only parameters, which determine the reaction rate. Therefore, the volumetric fuel consumption rate is given by:

$$\bar{\omega} = -\bar{\rho}A\left(\frac{\varepsilon}{k}\right)\min\left(\tilde{Y}_F, \frac{\tilde{Y}_O}{S_O}, \frac{B\tilde{Y}_P}{1+S_O}\right), \tag{Eq 1}$$

where $\bar{\omega}$ is the mean volumetric fuel consumption rate, and Y_F , Y_O , and Y_P are the mass fraction of fuel, oxidizer and products. $S_O = n_O M_O / n_F M_F$, A and B are constants taken as 4 and 0.5, respectively (Ref 29). n and M represent number of moles and molar mass, and subscripts O and F count for Oxidant and Fuel. As it is discussed in the introduction section, there are two concerns with utilizing EDM in HVOF guns. Firstly, particle temperature provided by numerical simulations is much lower than experimental data; and secondly, some suspicious secondary combustion reactions in the supersonic jet outside of barrel are reported when using rich mixtures.

To overcome these shortcomings, new finite rate chemistry combustion models, like EDC model (Ref 40) is used here. This model can consider the effects of detailed chemical kinetics in turbulent flow. The EDC has been widely used for combustion modeling for a great variety of premixed and diffusion controlled combustion problems (Ref 41). In addition, the ability of finite rate EDC model in simulation of high speed reactive turbulent flow has been approved (Ref 42).

The EDC model assumes that the chemical reaction occurs in the areas that the dissipation of turbulence energy is considerably high. In turbulent flows, these areas are

placed in isolated, highly strained regions, occupying only a small fraction of the flow. The length scales of these regions are in comparison with Kolmogorov scale. These regions, which are named fine structures, are responsible for dissipation of turbulence into heat as well as mixing between reactants in molecular scale (Ref 32). In the aspect of numerical modeling, each computational cell is divided into two sub-zones: (1) the reacting fine structure and (2) the non-reacting bulk gas zone (surrounding fluid). The interaction between the fine structure and the surrounding fluid determines the overall mean combustion rate (Ref 41). The species mass transfer between the fine structure and surrounding fluid which is equal to species mean consumption/production rate, $\bar{\omega}_k$, which is obtained as (Ref 40):

$$\bar{\omega}_k = \bar{\rho} \frac{\gamma^2 \chi}{\tau^*} (Y_k^0 - Y_k^*), \tag{Eq 2}$$

where $\bar{\rho}$ is density, γ is the length fraction of cell occupied by fine structure, χ is the fraction of fine structure where reaction occurs, τ^* is the time scale for the mass transfer between the fine structure and the surrounding fluid, and Y_k is the mass fraction of species k . The superscripts $*$ and 0 denote fine structure and surrounding fluid quantities. τ^* and γ are calculated using the following equations (Ref 40):

$$\tau^* = \left(\frac{C_{D2}}{3}\right)^{1/2} \left(\frac{\nu^*}{\varepsilon}\right)^{1/2}, \tag{Eq 3}$$

$$\gamma = \left(\frac{3C_{D2}}{4C_{D1}^2}\right)^{1/4} \left(\frac{\nu^* \varepsilon}{k^2}\right)^{1/4}, \tag{Eq 4}$$

where k is the turbulent kinetic energy, ε is the dissipation rate of turbulent kinetic energy, ν is the kinematic viscosity of the gas, and C_{D1} and C_{D2} are the model constant equal to 0.134 and 0.5, respectively (Ref 40). The mass fraction of species k in the surrounding fluid, Y_k^0 , can be related to the mass fraction of fine structure, Y_k^* and the mean mass fraction of computational cell, \bar{Y}_k , as:

$$Y_k^0 = \frac{\bar{Y}_k - \gamma^3 \chi Y_k^*}{(1 - \gamma^3 \chi)}. \tag{Eq 5}$$

Gran and Magnussen (Ref 40) demonstrated that the assumption $\chi = 1$ leaves the results almost unaltered.

To calculate the species mass fraction, Y_k^* , the fine structure is treated as an unsteady perfectly stirred reactor (PSR) with constant pressure and enthalpy. In fact, the effects of chemical kinetics are appeared implicitly in EDC model when the mass fraction of species k in the fine structure is taken into account. The set of governing equations for the fine structure reactor is (Ref 40):

$$\frac{dp^*}{dt} = 0, \quad (\text{Eq 6})$$

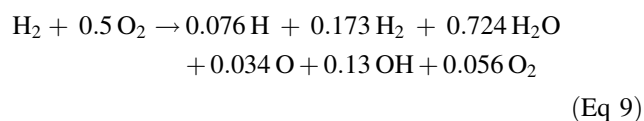
$$\frac{dh^*}{dt} = 0, \quad (\text{Eq 7})$$

$$\frac{dY_k^*}{dt} = \frac{\dot{\omega}_k^*}{\bar{\rho}} + \frac{1}{\tau^*} (Y_k^0 - Y_k^*), \quad (\text{Eq 8})$$

where $\dot{\omega}_k^*$ is the consumption/production rate of species k in the fine structure reactor which is determined during the chemistry calculations. The above set of ODE equations is integrated over a time scale of τ^* which represents the residence time inside the reactor.

In the present study, three different chemical kinetic mechanisms for hydrogen–oxygen mixture, consist of 7-step, 14-step and 21-step have been utilized in the EDC simulations. These mechanisms are taken from Ref 42–44. When using detailed chemical mechanisms along with EDC model, $\dot{\omega}_k^*$ in Eq 8 is obtained by solving a stiff ODE system. In the context of complex reacting flows, a large number of computational cells and time steps are required. This leads to an enormous amount of direct integrations of ODEs. Thus, a significant portion of the total time is dedicated to solving the kinetics equations. To overcome this drawback, the In Situ Adaptive Tabulation (ISAT) method, proposed by Pope (Ref 45) is used in the present work. In this tabulation procedure, the table is constructed during the simulation. The ISAT error tolerance which should adjusted by user is studied here. Three different thresholds (i.e., 10^{-3} , 10^{-4} and 10^{-5}) are examined as ISAT error tolerance. Since the gas and particle phase temperature diagrams are independent of the ISAT error tolerance in this range, the 10^{-3} is considered to reduce the computational cost.

It should be mentioned that using a multi-step reaction mechanism with the EDM model leads to incorrect solutions because multi-step reaction mechanisms are based on Arrhenius rates, which differ for each reaction. In the EDM, every reaction has the same, turbulent rate, and therefore the model should be used only for one-step, or two-step global reactions (Ref 36). Since the effect of chemical kinetics is ignored by EDM, the effects of intermediate species and dissociation reactions should be considered in order to avoid the over-prediction of temperature (Ref 15). To do this, a chemical equilibrium program (Ref 46) was used and following global one-step chemical equation was obtained for a stoichiometric hydrogen–oxygen mixture:



The above equation was obtained by minimizing the Gibbs free energy of combustion products under constant enthalpy and constant pressure. The pressure in the combustion chamber of warm spray using stoichiometric mixture is around 4 bars for the present operating conditions. Under these constraints, the intermediate species in the products composition remain unchanged, since any change in product composition will violate the second law of thermodynamics.

For hydrogen–oxygen mixture with other equivalence ratios, the similar calculation procedure was adopted.

Grid Study

For the purpose of grid study the temperature and velocity of gas phase for four different grids with 14,000, 55,000, 100,000, and 220,000 cells have been tested. For this purpose, EDC and RSM closure models are considered here. It is found that gas velocity is less sensitive to the grid density than temperature. In addition, while there is considerable difference between the gas phase temperature of grids with 14,000, 55,000 and 100,000, the temperature diagram of 220,000 cells fits the counterpart diagram of the grid with 100,000 cells. Thus, grid with 100,000 cells has been used for modeling the combustion-assisted process in the warm spray gun.

Results and Discussion

Validation

Since there is no published experimental or numerical data in the literature for the hydrogen-fueled warm spray gun, for validation purpose we model a propylene-fueled warm spray system introduced by Khan and Shamim (Ref 26) using EDM combustion model and $k-\epsilon$ RNG turbulence model. The particle temperature and particle velocity obtained in the current study compare with the results of Ref 26 in Fig. 3. As it can be seen, a very good agreement between the two results is achieved. Moreover, as it is mentioned by Tabbara et al. (Ref 25), using an advanced turbulence model such as RSM is preferred in numerical simulations of the warm spray. With this choice, the model can more realistically predict the mixing process of the cooling nitrogen gas with the combustion products. Hence, the results of EDM along with RSM model are included in Fig. 3 to compare with results obtained from $k-\epsilon$ RNG model. Although the discrepancy is minor, one may conclude that compared to the RSM model, utilizing $k-\epsilon$ RNG model leads to a higher prediction of the particle temper-

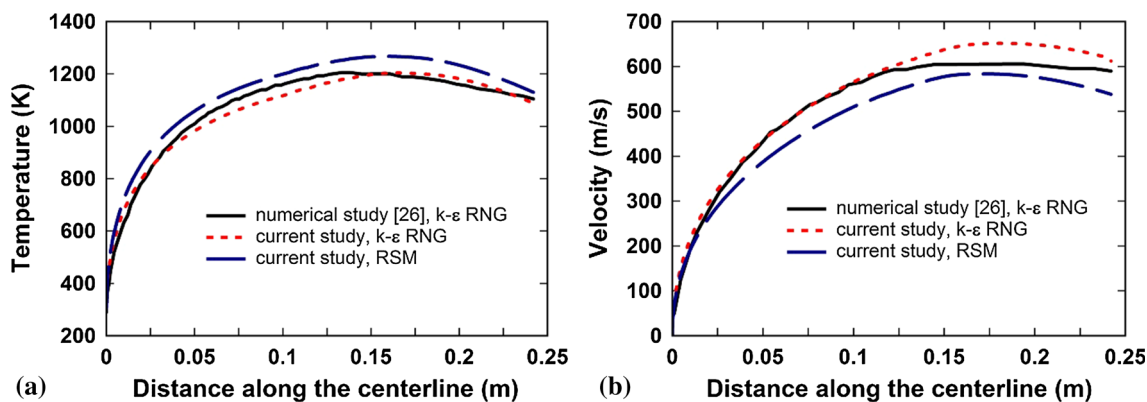


Fig. 3 Comparison of (a) temperature and (b) velocity of the particle phase as a function of distance along the centerline obtained in the present work against the numerical results of Ref 26

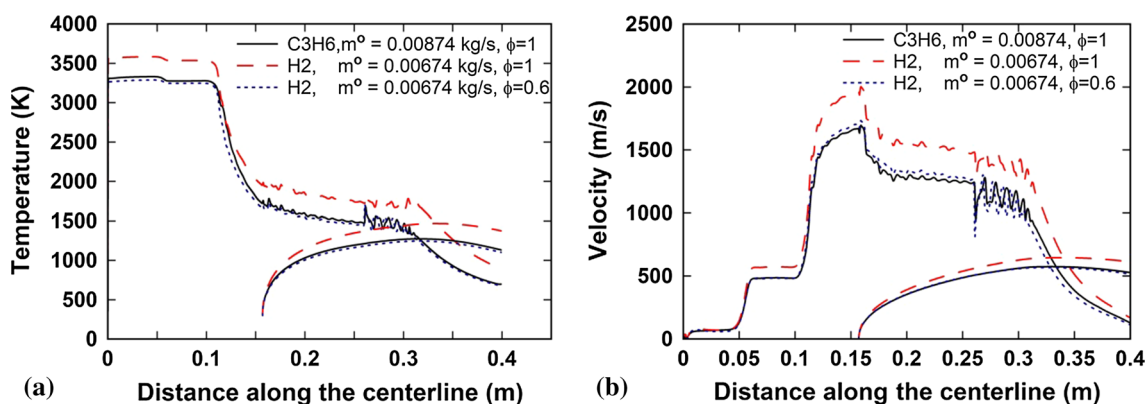


Fig. 4 Comparison of gas and particle temperature (a) and velocity (b) between propylene-fueled and hydrogen-fueled warm spray system. The particles are injected at $x = 157$ mm

ature and lower prediction of the particle velocity. Since compared to the $k-\epsilon$ RNG model, the RSM is a superior turbulence model, in the remainder of the paper result of the RSM model are presented and discussed.

Comparison Between Hydrogen- and Propylene-Fueled Warm Spray Systems

Figure 4 shows temperature and velocity profiles for gas and particle phases along the centerline of the geometry consider in Fig. 2, for one propylene-fueled and two hydrogen-fueled systems. As it can be seen in Fig. 4(a), the gas temperature in the combustion chamber increases due to combustion process (around 3300 K for propylene case). This high level of internal energy converts to kinetic energy when the exhaust gases accelerate through the converging and then C–D nozzles. In the C–D nozzle, the flow accelerates and becomes supersonic. Therefore, the flow experiences a drastic decline in pressure and temperature. When the supersonic flow comes out of the barrel, the diamond-like wave patterns with compression and

expansion waves form at downstream of the barrel exit (Ref 47). This complicated structure causes the gas velocity and temperature to undergo a series of fluctuations as seen in Fig. 4. The gas dynamic behavior of the hot supersonic jet produced by a conventional HVOF gun was studied in detail using optical diagnostic techniques in work by Hackett et al. (Ref 48).

As it is mentioned in Ref 1, the total pressure in the mixing chamber is an important parameter determines the gas dynamics behavior of flow in the C–D nozzle and barrel. Thus, for comparison purpose, the mass flow rate of reactant for hydrogen-fueled system is adjusted in order to have a total pressure in the mixing chamber the same as that for the propylene-fueled system. Although the reactant mass flow rate of propylene-fueled case is 0.00874 kg/s (Ref 26) by parametric study, it is conducted that the hydrogen-fueled case with reactant mass flow rate of 0.00674 kg/s will provide the total pressure in the mixing chamber similar to that of the propylene-fueled case when the equivalence ratio is $\phi = 1$. It should be mentioned that the turbulence and combustion models, mesh density,

equivalence ratio, ϕ , and other computational elements are the same for two fuel cases.

Figure 4(a) shows that for both cases with $\phi = 1$, hydrogen gun provides gas phase and particle phase temperatures to be 320 and 250 K higher than propylene-fueled system. This issue can be justified by the fact that hydrogen heat value per kilogram is much higher (around three times) than propylene. In combustion chamber, the temperature produced by hydrogen is 3600 K, while in propylene-fueled system it is 3300 K.

Figure 4(b) shows the velocity variation along the centerline for gas and particle phases for two systems. The velocity of gas and particle phases of hydrogen case is approximately 250 and 50 m/s higher than those for propylene-fueled case, respectively. Despite the fact that total pressure in the mixing chamber is the same for both systems, lower density of exhaust gases resulted from hydrogen combustion provided this higher velocity. The issue of lower flue gas density in hydrogen case also explains why 250 m/s higher gas phase velocity only provides 50 m/s higher particle phase velocity. In fact, higher flow density in propylene case increases the momentum exchange between the gas and particle phases and could roughly compensate the effect of 250 m/s lower gas velocity, compared with hydrogen-fueled case.

Figure 4 also reveals that hydrogen fuel with $\phi = 0.6$ (dotted blue lines) provides particle temperature and velocity the same as propylene case with $\phi = 1$ (solid back lines). While using hydrogen, the same velocity and temperature as propylene can be maintained if the equivalence ratio is decreased. In “EDC model versus EDM” and “Detailed versus reduced chemical kinetics” sections, it will be thoroughly discussed that for rich mixtures, while an increase in equivalence ratio reduces the particle temperature, it increases the particle velocity. Thus, one may conclude that rich mixtures are more desirable than lean mixtures to be considered for warm spray guns since for coating of phase-sensitive and temperature-sensitive materials like titanium lower temperature and higher velocity is desirable.

EDC Model Versus EDM

In this section, we take the advantage of EDC combustion model in order to investigate some previously observed and reported phenomena in numerical studies of HVOF guns (as discussed in introduction section). For this purpose, the detailed H₂-air chemical reaction mechanism containing 9 species and 21 steps (Ref 44) is utilized with the EDC model in order to take into account the impact of chemistry in a hydrogen-fueled warm spray system.

Figure 5(a) displays the temperatures of gas and particle phases obtained from EDM and EDC computations for

both stoichiometric ($\phi = 1$) and rich mixtures ($\phi = 1.4$) for the hydrogen-fueled system. Since EDM model with global one-step reaction mechanism ignores elementary reactions and chemical kinetic rates, it is usually expected that this model over-predicts the combustion temperature in highly turbulent regions (Ref 29). Accordingly, the results of Fig. 5(a) show that gas temperature in the combustion chamber and mixing chamber calculated by EDM theory is around 300 K higher than EDC model (for $\phi = 1$). However, the temperature of gas in the C–D nozzle, barrel and exit of barrel, and particle phase temperature obtained using EDM model are lower than those of EDC model. In fact, concurrently entering the C–D nozzle some elementary exothermic reactions, which are present in detailed chemical mechanism of H₂-air mixture, initiate and give rise to temperature in this section. In other words, the exothermic reactions which are mostly responsible for producing water (especially: $\text{H}_2 + \text{OH} \rightarrow \text{H}_2\text{O} + \text{H}$) are activated in this section and increase the gas phase temperature significantly. This issue provides the gas phase temperature of the EDC around 300 K higher than EDM in the barrel.

According to Fig. 5(a), another noticeable difference between results of EDM and EDC models is a considerable increase in gas phase and consequently particle phase temperatures for rich mixture ($\phi = 1.4$) outside of barrel (in atmospheric air) when utilizing EDM combustion scheme. In EDM, gas phase temperature of rich mixture is lower than stoichiometric mixture until around $x = 317$ mm (60 mm outside of barrel). Slightly before $x = 317$ mm, a sudden increase by 500 K in gas phase temperature is observed. This increase in gas temperature causes a rise in particle temperature with a slight delay and results in crossing particle temperature of the stoichiometric mixture. This extra heat release is observed by many researchers (Ref 8, 27, 30) who utilized turbulence limited combustion models along with rich mixtures. This is justified by diffusion of ambient air into the core of supersonic jet and burning of unburned fuels. However, flow velocity, temperature in this region, and low concentration of fuel makes this amount of heat release unlikely and unphysical. On the other hand, EDC theory better controls these reactions and provides more realistic results. As it can be seen in Fig. 5(a), for EDC model, there is no extreme increase in the gas temperature outside of barrel. Indeed, in EDC model, the fact that gas temperature of rich mixture (dashed blue line) crosses the stoichiometric mixture (constant blue line) at $x = 375$ mm, confirms the presence of some exothermic reactions outside of the barrel. Nonetheless, this heat release is not as severe as EDM predicts. In other words, the heat release outside of barrel is minor, and neither the gas phase nor the particle phase is affected by these reactions significantly. This issue also

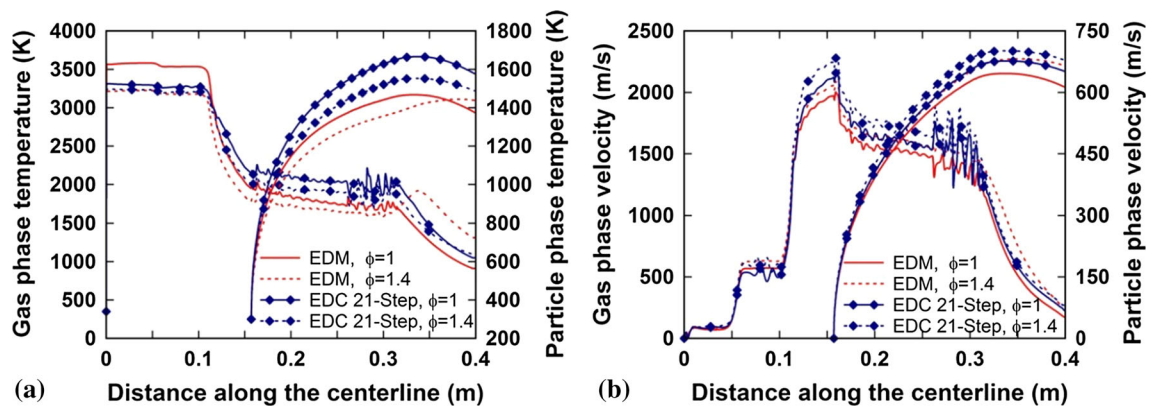


Fig. 5 The impact of EDM and EDC modeling of combustion in a hydrogen-fueled warm spray system on gas and particle (a) temperature and (b) velocity

will be more discussed in “Detailed versus reduced chemical kinetics” section.

Finally, we can conclude that EDM modeling of combustion in warm spray under-predicts temperatures of the gas and particle phases. By comparing the particle temperature predicted by EDC and EDM models for stoichiometric mixtures, we see that the particle temperature at the end of the computational domain for EDC is 200 K (i.e., 13%) higher than those of EDM. For gas phase temperature, this difference is around 150 K (i.e., 16%). The differences between EDM and EDC for rich mixture ($\phi = 1.4$) are approximately 50 K (i.e., 4%) and 300 K (i.e., 30%) for particle and gas phase temperatures, respectively. Regarding particle temperature, the difference between EDM and EDC for rich mixture is small because some unphysical reactions outside of barrel in EDM, give rise to the temperatures of the gas and particle phases. Thus, the particle temperature (dashed red line) from EDM comes close to that of EDC (dashed blue line). It can be concluded that the EDC theory better represents the nature of problem in the HVOF system since previously utilized turbulence limiting combustion models suffered lack of accuracy by under predicting the particle temperature (Ref 8, 19, 26).

Figure 5(b) shows that for both stoichiometric and rich mixtures, EDC model predict the gas velocity around 100 m/s higher than those of EDM in the barrel. EDC also predicts the particle velocity around 40 m/s higher.

Another issue, which is evident in the results for both temperature and velocity of gas phase, is the fact that in EDM we have an over-expanded flow outside of the barrel. This over-expansion is characterized by the existence of a shock wave at the barrel exit, which features itself as a reduction in velocity and an increase in temperature profiles (red lines) in Fig. 5. However, the EDC model presents an under-expanded flow in this section. This is because the heat addition in the C–D nozzle in EDC model

delays the over-expansion of the flow, and even can result in an under-expanded flow.

Detailed Versus Reduced Chemical Kinetics

In this section, the results of EDM with global one-step reaction mechanism are compared with EDC model along with 21-step detailed chemical kinetics (Ref 44) and two reduced chemical kinetics for hydrogen–oxygen mixture. The first reduced reaction mechanism involves seven species and seven reversible reactions. This mechanism includes the species H_2 , O_2 , H_2O , O , OH , H , and N_2 (Ref 42). The second reduced reaction mechanism contains nine species and fourteen elementary reactions (Ref 43). In fact, both 21-step (Ref 44) and 14-step mechanisms (Ref 43) consider two more species, HO_2 and H_2O_2 . The main objective in this section is to compare the capability of the two reduced mechanisms with the detailed one in predicting the flow feature in a hydrogen-fueled system. In fact, the computational cost of utilizing detailed kinetics like Li et al. (Ref 44) is very high, and the necessity of using such a detailed kinetics should be examined.

Figure 6(a) shows the maximum particle temperature in different equivalence ratios for EDM and EDC models with three chemical mechanisms. As explained before, it is seen that EDM model fails to predict the decreasing trend the particle temperature in the rich mixtures and an increasing trend is observed for equivalence ratios greater than 1.4. For EDC model, the three chemical mechanisms predict almost similar behavior for maximum particle temperature as a function of equivalence ratio. However, the equivalent ratios which the maximum temperature is highest, are different for three mechanisms. For 7-step and 14-step this occurs at $\phi = 1$, while for 21-step this occurs at $\phi = 1.2$.

Although EDM predicts the increasing trend of the maximum particle temperature until $\phi = 1$, it cannot

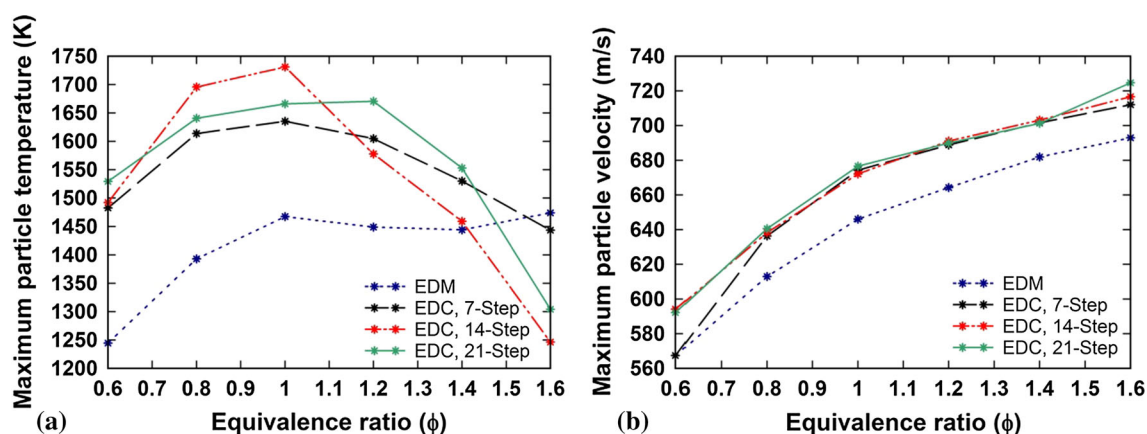


Fig. 6 Maximum particle temperature (a) and velocity (b) for EDM and EDC along with three distinct kinetics in different equivalence ratios for hydrogen–oxygen mixture. The particles are injected at $x = 157$ mm

predict accurately the decreasing trend of maximum temperature for higher equivalence ratios. In addition, even for lean mixtures, the maximum particle temperature predicted by EDM is about 17% lower than that of EDC model.

The results of 21-step mechanism are in good agreement with the experimental results of Turunen et al. (Ref 31) running the single-stage HVOF with hydrogen fuel. They reported that the highest temperature was obtained by using the equivalence ratio slightly above 1.2. Although all three mechanisms lead to decrease in particle maximum temperature for mixtures richer than 1.2, the intensity of this reduction varies for different mechanisms.

Figure 6(b) describes the maximum particle velocity of EDM and EDC with three different mechanisms as a function of equivalence ratio, ϕ . It is seen that the maximum velocity of particle in both EDM and EDC simulation increases as the ϕ increases. However, the particle velocity predicted in EDM model is about 30 m/s (i.e., 5%) lower than those predicted using all three EDC cases. In addition, it is seen that the velocity diagrams of all three mechanisms overlaps, especially for $\phi > 0.8$. This shows that different mechanisms predict different maximum particle temperature, while they predict almost similar maximum velocities for particle phase.

One valuable conclusion which can be derived from Fig. 6 is the fact that, by moving to rich mixtures the temperature of particles decreases, while their velocity increases. Both of these characteristics (lower temperature and higher velocity) are highly desirable in warm spray technology (Ref 1). This issue has high order of significance since it shows that moving toward rich mixtures is not only a way of controlling (lowering) the particle temperature but also is more advantageous than moving toward lean mixture because utilizing lean mixture will reduce both particle velocity and temperature. This conclusion is against those who utilized EDM turbulence limited

combustion models in their research. Khan and Shamim (Ref 27) used EDM in a dual-stage HVOF system, and concluded that increase in equivalence ratio will result in increase in particle temperature. Shamim et al. (Ref 8) and Baik and Kim (Ref 30) utilized EDM in modeling of single-stage HVOF gun. They also reported increase in particle temperature while using rich mixtures.

Another significant point which should be emphasized in this section is the fact that EDC with the multi-step reaction mechanism was successful in providing higher particle temperature and velocity. To the best of our knowledge, there is no experimental data in the literature on the hydrogen-fueled warm spray technology to comment on the validation of these findings. However, Shamim et al. (Ref 8), Dolatabadi et al. (Ref 19), and Khan and Shamim (Ref 26) failed in fitting the experimental data from a single-stage, propylene-fueled HVOF system. The findings of this section implicitly prove that EDC along with multi-step reaction mechanisms and RSM turbulence model better presents the nature of process in the HVOF gun.

Nonetheless, from the results given in “EDC model versus EDM” and “Detailed versus reduced chemical kinetics” sections, one may conclude that EDM has a reasonable capability in predicting the temperature and velocity fields in the HVOF system in lean mixtures (about 5 and 17% under-prediction for velocity and temperature compared to the EDC model). However, the conventional HVOF systems usually run with slightly rich mixture to avoid oxidation of inflight particles (Ref 11). Although the EDM fails to predict the increasing trend of the particle maximum temperature for rich mixtures, due to lower computational cost and easier convergence, it can be a preferred model to parametric studies in a limited range of equivalence ratios as the qualitative trend is correctly predicted.

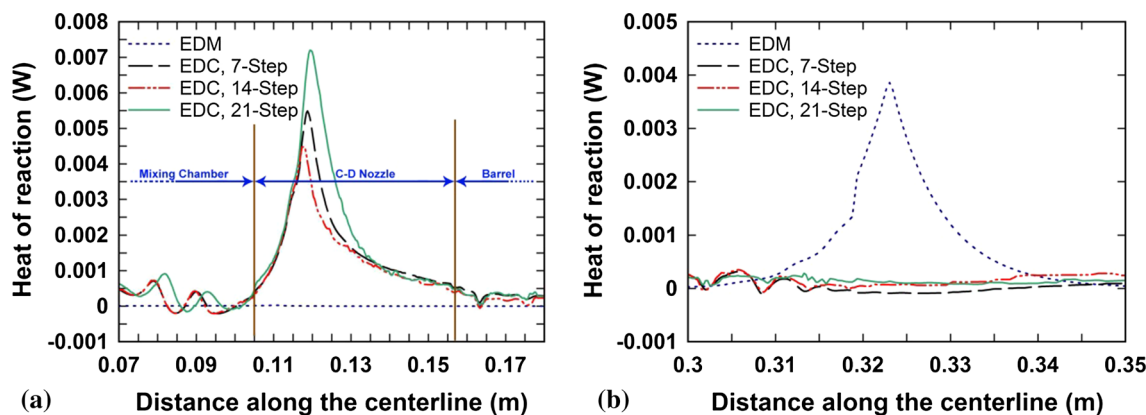


Fig. 7 Amount of heat release on the centerline for the slightly rich mixture with $\phi = 1.2$, (a) for region between $x = 70$ mm to $x = 180$ mm and (b) for region between $x = 300$ mm to $x = 350$ mm

Heat of Reaction for EDC and EDM Models

In this section, the amount of heat release at different sections of the warm spray gun is discussed. Figure 7 shows the amount of heat release of slightly rich mixture ($\phi = 1.2$) on the centerline for EDC along with three mechanisms and also EDM model at different sections. Figure 7(a) shows the heat release with focus on the range of $x = 70$ mm to $x = 180$ mm. This range covers the mixing chamber, the C–D nozzle, and beginning part of the barrel. All EDC simulations reveal the presence of some exothermic reactions, which are initiated entering C–D nozzle and reach to their pick near the throat of nozzle. However, the EDM combustion model with the global one-step reaction mechanism completely ignores the exothermic reactions throughout the region and thus cannot predict the heat of reaction accurately. Since the EDM is a turbulence limited combustion model, most of the heat release in EDM simulation occurs at the beginning of the combustion chamber where the premixed hydrogen–oxygen mixture enters the computational domain (note that the oxy-fuel mixture enters at 3 mm above the centerline). In fact, EDM model produces locally high temperature at oxy-fuel entrance section. On the other hand, EDC model takes into account the impact of chemical kinetics, and mixing is not the only parameter, which controls the rate of combustion and heat release in the combustion chamber. Therefore, it is expected that for all mechanisms (7-step, 14-step, and 21-step) heat release be distributed (not evenly) in all region of the combustion chamber.

Figure 7(b) depicts the heat of reaction for EDC and EDM models in the region between $x = 300$ mm and $x = 350$ mm which is outside of the barrel. This figure shows that all the three chemical kinetics of EDC model produce no significant heat of reactions outside of the barrel, while EDM model shows significant amount of

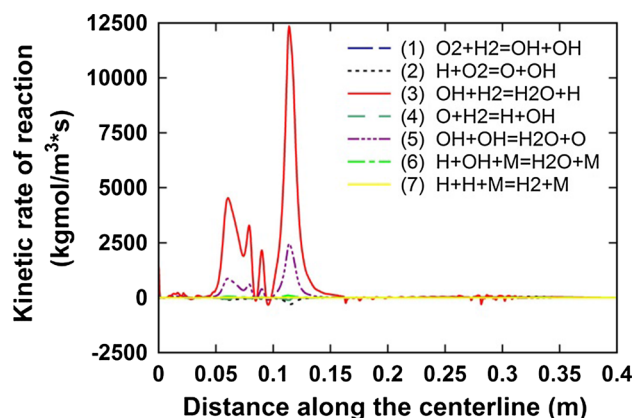


Fig. 8 Rate of different elementary reactions of 7-step mechanism on the centerline

heat being released in this section. In fact, there are two shortcomings with EDM model. First, this model over-predicts the reaction rate in highly strained regions where ε/k ratio is high (mixing time scale is low) (Ref 29), and this can cause artificial flame to be observed. Second, this model predicts similar reaction rate at regions with similar species concentration and turbulence level but different temperatures. These weaknesses cause the artificial heat release to be observed outside of the barrel. In fact, high speed of flow, low concentration of fuel and oxygen and low temperature prevent this large amount of exothermic combustion reactions.

Figure 8 depicts the kinetic rate of 7 reactions, which are involved in 7-step mechanism (Ref 42) in order to discuss the issue of heat release through C–D nozzle in EDC model. The reason why the 7-step reaction mechanism has been used is that investigation and comparison between the behaviors of kinetics with high number of elementary reactions is a little bit confusing especially if all of the reactions are plotted on one graph. As it can be seen in Fig. 8, the exothermic reactions which are responsible

for producing H_2O (reactions number 3, 5 and 6) are activated at this section. Especially, reaction number 3 ($OH + H_2 = H_2O + H$) has a giant increase at this section. These chain terminating reactions are responsible for the heat release in middle of C–D nozzle (see Fig. 7a) which is discussed previously.

Conclusions

Taking advantage of EDC combustion theory along with detailed and reduced reaction mechanisms and RSM turbulence model, the physics underlying the warm spray process and combustion-related underlying factors has been investigated. The findings of this research can be considered both as a response to previously raised concerns regarding the effectiveness of numerical modeling in the single- and dual-stage HVOF guns and an efficient tool for improving the accuracy of future researches. These findings are as follows:

- The impact of chemistry of combustion should be considered for accurate estimation of particle temperature. Ignoring the chemistry will lead to disassemble the exothermic reactions in the C–D nozzle and cause underestimation of gas and particle temperatures.
- Heat addition to the flow by exothermic reactions will delay the over-expansion and even cause the under expansion of gas at the barrel exit.
- EDC reveals that by moving to rich mixtures the temperature decreases while the velocity increases and both of characteristics (lower temperature and higher velocity) are desirable for coating of phase-sensitive and temperature-sensitive materials like titanium.
- While the nature of considering chemistry of combustion affects the particle temperature, the velocity of particle is almost independent of the kind of multi-step mechanism which has been used in EDC model.
- While EDM shows drastic increase in the gas and particle temperatures outside of barrel when rich mixture is used, EDC theory does not show significant heat release outside of barrel. Thus, the gas and the particle temperatures are not affected by such secondary reactions.

Open Access This article is distributed under the terms of the Creative Commons Attribution 4.0 International License (<http://creativecommons.org/licenses/by/4.0/>), which permits unrestricted use, distribution, and reproduction in any medium, provided you give appropriate credit to the original author(s) and the source, provide a link to the Creative Commons license, and indicate if changes were made.

References

1. S. Kuroda, J. Kawakita, M. Watanabe, K.H. Kim, R. Molak, and H. Katanoda, Current Status and Future Prospects of Warm Spray Technology, *Future Development of Thermal Spray Coatings: Types, Designs, Manufacture and Applications*, 1st ed., N. Espallargas, Ed., Woodhead Publishing, Sawston, 2015, p 163–206
2. M. Li and P.D. Christofides, Modeling and Control of High-Velocity Oxygen-Fuel (HVOF) Thermal Spray: A Tutorial Review, *J. Therm. Spray Technol.*, 2009, **18**, p 753–768
3. H. Jafari, S. Emami, and Y. Mahmoudi, Numerical Investigation of Dual-Stage High Velocity Oxy-fuel (HVOF) Thermal Spray Process: A Study on Nozzle Geometrical Parameters, *Appl. Therm. Eng.*, 2017, **111**, p 745–758
4. J. Kawakita, S. Kuroda, T. Fukushima, H. Katanoda, K. Matsuo, and H. Fukunuma, Dense Titanium Coatings by Modified HVOF Spraying, *Surf. Coat. Technol.*, 2006, **201**, p 1250–1255
5. X. Yang and S. Eidelman, Numerical Analysis of a High-Velocity Oxygen-Fuel Thermal Spray System, *J. Therm. Spray Technol.*, 1996, **5**, p 175–184
6. J. Mostaghimi, S. Chandra, R. Ghafouri-Azar, and A. Dolatabadi, Modeling Thermal Spray Coating Processes: A Powerful Tool in Design and Optimization, *Surf. Coat. Technol.*, 2003, **163**, p 1–11
7. E. Dongmo, M. Wenzelburger, and R. Gadow, Analysis and Optimization of the HVOF Process by Combined Experimental and Numerical Approaches, *Surf. Coat. Technol.*, 2008, **202**, p 4470–4478
8. T. Shamim, C. Xia, and P. Mohanty, Modeling and Analysis of Combustion Assisted Thermal Spray Processes, *Int. J. Therm. Sci.*, 2007, **46**, p 755–767
9. G.D. Power, T.J. Barber, and L.M. Chiappetta, *Analysis of High Velocity Oxygen Fuel (HVOF) Thermal Torch*, American Institute of Aeronautics and Astronautics, 1992, Paper No. 92-3598
10. E.B. Smith, G.D. Power, T.J. Barber, and L.M. Chiappetta, Application of Computational Fluid Dynamics to the HVOF Thermal Spray Gun, *Thermal Spray: International Advances in Coatings Technology*, C.C. Berndt, Ed., ASM International, Almere, 1992, p 805–810
11. C.H. Chang and R.L. Moore, Numerical Simulation of Gas and Particle Flow in a High-Velocity Oxygen-Fuel (HVOF) Torch, *J. Therm. Spray Technol.*, 1995, **4**, p 358–366
12. B. Hassan, W.L. Oberkampf, R.A. Neiser, A.R. Lopez, and T.J. Roemer, *Computational and Experimental Investigation of High-Velocity Oxygen-Fuel (HVOF) Thermal Spraying*, American Institute of Aeronautics and Astronautics, 1996, Paper No. 96-1939
13. A.R. Lopez, B. Hassan, W.L. Oberkampf, R.A. Neiser, and T.J. Roemer, Computational Fluid Dynamics Analysis of a Wire-Feed, High-Velocity Oxygen Fuel (HVOF) Thermal Spray Torch, *J. Therm. Spray Technol.*, 1998, **7**(3), p 374–382
14. S. Gu, C.N. Eastwick, K.A. Simmons, and D.G. McCartney, Computational Fluid Dynamic Modeling of Gas Flow Characteristics in a High-Velocity Oxy-Fuel Thermal Spray System, *J. Therm. Spray Technol.*, 2001, **10**(3), p 461–469
15. W.L. Oberkampf and M. Talpallikar, Analysis of a High-Velocity Oxygen-Fuel (HVOF) Thermal Spray Torch Part 1: Numerical Formulation, *J. Therm. Spray Technol.*, 1996, **5**(1), p 53–61
16. B. Hassan, A.R. Lopez, and W.L. Oberkampf, Computational Analysis of a Three-Dimensional High-Velocity Oxygen Fuel (HVOF) Thermal Spray Torch, *J. Therm. Spray Technol.*, 1998, **7**, p 71–77
17. D. Cheng, Q. Xu, E. Lavernia, and G. Tapaga, The Effect of Particle Size and Morphology on the In-Flight Behavior of

- Particles During High Velocity Oxy-Fuel Thermal Spraying, *Metall. Mater. Trans. B*, 2001, **32**, p 525-535
18. D. Cheng, Q. Xu, G. Tapaga, and E. Lavernia, A Numerical Study of High-Velocity Oxygen Fuel Thermal Spraying Process. Part I: Gas Phase Dynamics, *Metall. Mater. Trans. A*, 2001, **32**, p 1609-1620
 19. A. Dolatabadi, J. Mostaghimi, and V. Pershin, Effect of a Cylindrical Shroud on Particle Conditions in High Velocity Oxy-Fuel (HVOF) Spray Process, *J. Mater. Process. Technol.*, 2002, **137**, p 214-224
 20. M. Li and P.D. Christofides, Multi-Scale Modeling and Analysis of an Industrial HVOF Thermal Spray Process, *Chem. Eng. Sci.*, 2005, **60**, p 3649-3669
 21. M. Li, D. Panagiotis, and P.D. Christofides, Computational Study of Particle In-Flight Behavior in the HVOF Thermal Spray Process, *Chem. Eng. Sci.*, 2006, **61**, p 6540-6552
 22. S. Kamnis and S. Gu, 3-D Modelling of Kerosene-Fuelled HVOF Thermal Spray Gun, *Chem. Eng. Sci.*, 2006, **61**, p 5427-5439
 23. S. Kamnis and S. Gu, Numerical Modelling of Propane Combustion in a High Velocity Oxygen-Fuel Thermal Spray Gun, *Chem. Eng. Process.*, 2006, **45**, p 246-253
 24. H. Tabbara and S. Gu, Computational Simulation of Liquid-Fuelled HVOF Thermal Spraying, *Surf. Coat. Technol.*, 2009, **204**, p 676-684
 25. H. Tabbara, S. Gu, and D.G. McCartney, Computational Modeling of Titanium Particles in Warm Spray, *Comput. Fluid*, 2011, **44**, p 358-368
 26. M.N. Khan and T. Shamim, Investigation of a Dual-Stage High Velocity Oxygen Fuel Thermal Spray System, *Appl. Energy*, 2014, **130**, p 853-862
 27. M.N. Khan and T. Shamim, Effect of Operating Parameters on a Dual-Stage High Velocity Oxygen Fuel Thermal Spray System, *J. Therm. Spray Technol.*, 2014, **23**, p 910-918
 28. M.N. Khan and T. Shamim, Effect of Particle and Injection Parameters on the Performance of a Dual-Stage High-Velocity Oxygen Fuel Thermal Spray System, *J. Therm. Spray Technol.*, 2015, **24**, p 807-816
 29. T. Poinsoot and D. Veynante, *Theoretical and Numerical Combustion*, 2nd ed., R.T. Edwards Inc., Philadelphia, 2005
 30. J.S. Baik and Y.J. Kim, Effect of Nozzle Shape on the Performance of High Velocity Oxygen-Fuel Thermal Spray System, *Surf. Coat. Technol.*, 2008, **202**, p 5457-5462
 31. E. Turunen, T. Varis, S.P. Hannula, A. Vaidya, A. Kulkarni, J. Gutleber, S. Sampath, and H. Herman, On the Role of Particle State and Deposition Procedure on Mechanical, Tribological and Dielectric Response of High Velocity Oxy-Fuel Sprayed Alumina Coatings, *Mater. Sci. Eng. A*, 2006, **415**, p 1-11
 32. B.F. Magnussen, On the Structure of Turbulent and a Generalized Eddy Dissipation Concept for Chemical Reaction in Turbulent Flow, *19th American Institute of Aeronautics and Astronautics Aerospace Science Meeting, (Missouri, USA), January 12–15, 1981*
 33. X. Wang, Q. Song, and Z. Yu, Numerical Investigation of Combustion and Flow Dynamics in a High Velocity Oxygen-Fuel Thermal Spray Gun, *J. Therm. Spray Technol.*, 2016, **25**, p 441-450
 34. D.E. Crawmer, Thermal Spray Processes, *Handbook of Thermal Spray Technology*, 1st ed., J.R. Davis, Ed., ASM International, Almere, 2004, p 54-76
 35. E. Lugscheider, C. Herbst, and L. Zhao, Parameter Studies on High-Velocity Oxy-Fuel Spraying of MCrAlY Coatings, *Surf. Coat. Technol.*, 1998, **108–109**, p 16-23
 36. Fluent Inc., *Fluent Theory Guide*, Fluent Inc., New York, 2006
 37. H.K. Versteeg and W. Malalasekera, *An Introduction to Computational Fluid Dynamics*, 2nd ed., Prentice Hall, Loughborough, 2007
 38. Fluent Inc., *Fluent User's Guide*, Fluent Inc., New York, 2006
 39. B.F. Magnussen and B.H. Hjertager, On the Mathematical Modeling of Turbulent Combustion with Special Emphasis on Soot Formation and Combustion, *Proc. Combust. Inst.*, 1976, **16**, p 719-729
 40. I.R. Gran and B.F. Magnussen, A Numerical Study of a Bluff-Body Stabilized Diffusion Flame. Part 2. Influence of Combustion Modeling and Finite-Rate Chemistry, *Combust. Sci. Technol.*, 1996, **119**(1), p 191-217
 41. B.F. Magnussen, The Eddy Dissipation Concept a Bridge Between Science and Technology, *ECCOMAS Thematic Conference on Computational Combustion (Lisbon, Portugal), June 21–24, 2005*
 42. D. Chakraborty, P.J. Paul, and H.S. Mukunda, Evaluation of Combustion Models for High Speed H₂/air Confined Mixing Layer Using DNS Data, *Combust. Flame*, 2000, **121**, p 195-209
 43. B.D. Hitch, and D.W. Senser, Reduced H₂-O₂ Mechanisms for Use in Reacting Flow Simulation, *AIAA 26th Aerospace Sciences Meeting (Reno, Nevada, USA), January 11–14, 1988*
 44. J. Li, Z. Zhao, A. Kazakov, and F.L. Dryer, An Updated Comprehensive Kinetic Model of Hydrogen Combustion, *Int. J. Chem. Kinet.*, 2004, **36**, p 566-575
 45. S.B. Pope, Computationally Efficient Implementation of Combustion Chemistry Using In Situ Adaptive Tabulation, *Combust. Theory Model.*, 1997, **1**, p 41-63
 46. S. Gordon and B.J. McBride, *Computer Program for Calculation of Complex Chemical Equilibrium Compositions and Applications*, NASA Reference Publication 1311, Lewis Research Center, Cleveland, 1994
 47. J.D. Anderson, *Modern Compressible Flow: With Historical Perspective*, 3rd ed., McGraw-Hill, Singapore, 2003
 48. C.M. Hackett, G.S. Settles, and J.D. Miller, On the Gas Dynamics of HVOF Thermal Sprays, *J. Therm. Spray Technol.*, 1994, **3**, p 299-304